Cobra Maneuver Unsteady Aerodynamic Considerations

Lars E. Ericsson*
Mountain View, California 94040

Introduction

THE "COBRA" maneuver, performed by Pougachev at the 1989 Paris air show with the Soviet Su-27 "Flanker,"[1] and later performed also with a MiG-29 at the Canadian National Air Show in Ottawa,[2] requires lateral high-alpha stability superior to what until then had been demonstrated by other aircraft.[3] One conclusion that has been drawn is that somehow symmetric flow separation has to be assured through the alpha range $0 < \alpha < 120$ deg. Some attention has been given to the problem of preventing the vortices from highly swept wing leading edges from generating large lateral loads in roll and yaw through asymmetric vortex breakdown and/or vortex liftoff.[4,5] However, little has been said about the potentially more serious lateral stability problem presented by asymmetric flow separation from a slender forebody.[6,7] The lateral stability provided by the twin fins on the Russian aircraft[1,2] is probably comparable to that on U.S. aircraft, which have experienced uncontrollable yawing moments at $\alpha > 50$ deg.[6] The separation asymmetry on a slender forebody is controlled by so-called microasymmetries,[7] as has been demonstrated by the effect of roll angle on a pointed ogive.[8] The flow separation can be forced to be symmetric by the use of body strakes, trips, and by other means.[9] It is noted in Ref. 3 that "the Su-27 radome does have small chines located at the apex of the nose. These chines are small but probably have a very positive effect on high AOA stability." That chines may not always be successful in eliminating or even alleviating forebody flow asymmetry at zero side slip has been demonstrated in low-speed tests with conic noses.[10] In these tests a nose boom was found to reduce the maximum side force $|C_Y|_{max}$ more than lateral strakes located near the apex. However, this favorable nose-boom effect appears not to be present at higher Reynolds numbers.[8,9,11] Thus, not too much of an effect should be expected from the presence of nose booms on Su-27 and MiG-29. The vortex wake from the very slender nose boom embeds the apex of the forebody, possibly having an alleviating effect similar to that of nose bluntness.[9] Consequently, the experimental results for a blunted cone-cylinder geometry in rapid pitching motion[12] (Fig. 1) should be of some relevance.

Asymmetric Vortices on a Pitching Body

The pitch-rate-induced angle of attack at the nose tip is $-\bar{\alpha} = -\dot{\alpha}x_{CG}/U_\infty = -0.175 = -10$ deg for the pitch-up motion, and for the pitch-down case the angle of attack is increased by 10 deg (Fig. 1). Accounting for this pitch-rate-induced angle of attack (dashed lines in Fig. 2) did not fully account for the experimentally observed effect of the pitch rate on the boundaries between symmetric, asymmetric, and unsteady vortex shedding (solid lines in Fig. 2). However, it has been shown[13] that if one adds the time lag for convection of the pitch-rate-induced effect from the nose to the local station x, the predicted boundary in Fig. 2 will agree with the experimental data trend.[12] The message one obtains from the experimental results in Fig. 2 is that the large side forces with associated huge yawing moments experienced in static tests[6,11] should be realized also in a rapid pitching maneuver at laminar flow conditions. The 70 deg/s maximum pitch rate estimated for Su-27[3] would induce an angle of attack at the nose of less than 5 deg, i.e., well within the range covered in Fig. 2. Even when allowing for the fact that the asymmetric loads on the nose would be somewhat lower at the high Reynolds numbers of full-scale flight than at the laminar flow conditions of the

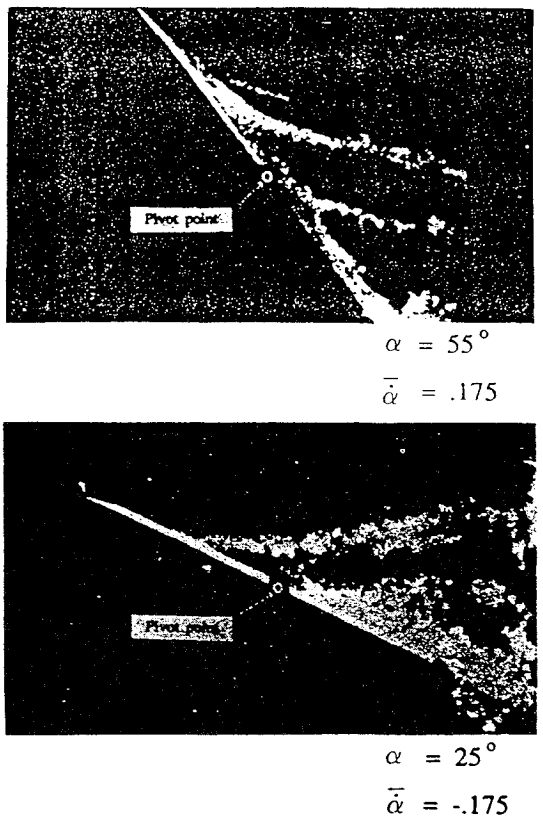

Fig. 1 Asymmetric vortices on cone-cylinder body in rapid pitch-up and pitch-down motions.[12]

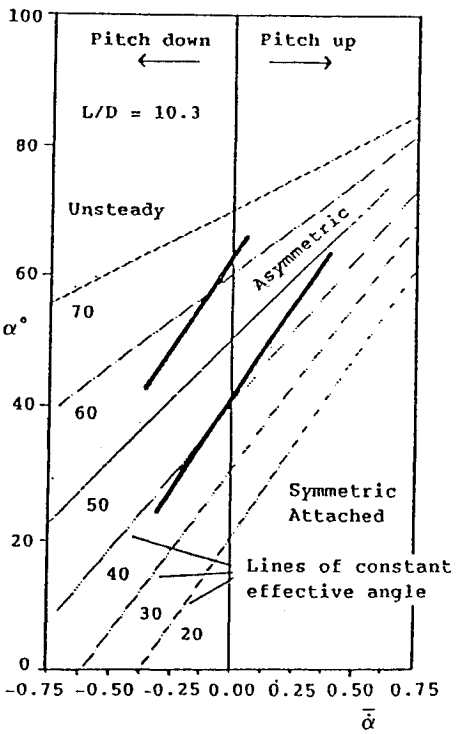

Fig. 2 Angle-of-attack/pitch-rate boundaries for symmetric, asymmetric, and unsteady vortex shedding.[12]

Received Feb. 7, 1993; revision received March 30, 1994; accepted for publication April 10, 1994.

*Engineering Consultant. Fellow AIAA.

ground test,[14] one would expect a situation qualitatively similar to the one illustrated in Fig. 2. Thus, based upon the experimental results discussed so far, the Su-27 and MiG-29 aircraft should have experienced significant out-of-plane moments. However, before one can say anything about nose-slice tendencies, one has to analyze the nose-slice motion and the associated moving wall effects.[15]

Experimental results[16] have shown how powerful the moving wall effects on laminar flow separation can be. They dominate completely over the effect of roll angle observed in static tests of a pointed ogive-cylinder at laminar flow conditions.[17] As the moving wall effects are concentrated to a region near the crossflow stagnation point,[18] the moving wall effects measured on a rotating circular cylinder[19] could be applied to the translating circular cross section of the coning body (see inset in Fig. 3), resulting in a predicted data trend[20] that agrees well with the experimental results.[16] This type of moving wall effect caused the observed lateral oscillations of sting-mounted slender-nosed models in ground tests at laminar flow conditions.[21] Assuming that lateral motion does develop during the pitch-up maneuver, similar moving wall effects will be present.

Self-Induced Coning Oscillation

It has been demonstrated that when the crossflow conditions become critical, the asymmetric flow separation on a pointed slender nose is the result of asymmetric boundary-layer transition.[22] The moving wall effect on flow separation via transition is responsible for the self-induced oscillatory coning observed on the cone-cylinder body (Fig. 3) when it was turned around 180 deg.[16,20] In this case a change of coning direction occurred without any external (even ever so subtle) forcing, in contrast to the case shown in Fig. 3. The Magnus lift measured on a rotating circular cylinder[19] shows the reason for this (Fig. 4). At $Re = 0.128 \times 10^6$, curve f in Fig. 4, so-called Magnus lift reversal occurs when $U_W/U_\infty > 0.3$. This is caused by the upstream moving wall effect on the bottom side, which, when the critical U_W/U_∞-Reynolds number combination is exceeded, will cause boundary-layer transition to occur upstream of flow separation, thereby changing the separation from the subcritical towards the supercritical type. This results in a more or less discontinuous loss of lift. This negative Magnus lift reaches its maximum magnitude when

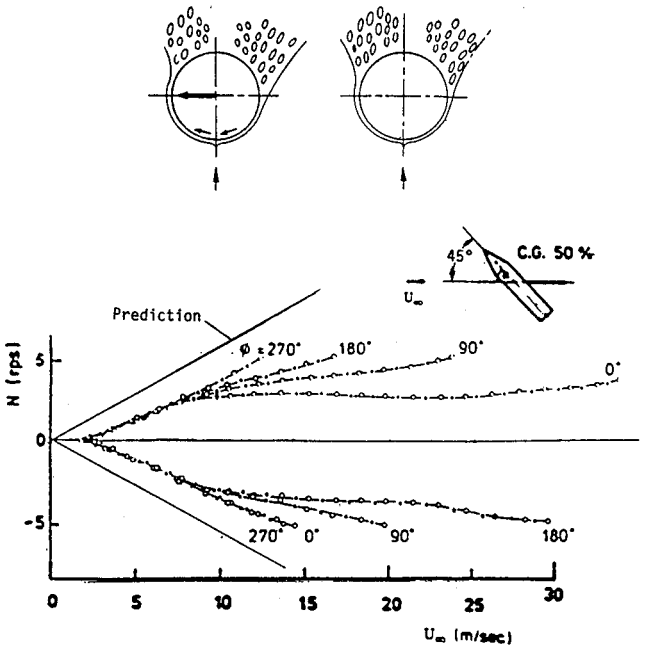

Fig. 3 Low-speed coning characteristics of a cone-cylinder body.[16]

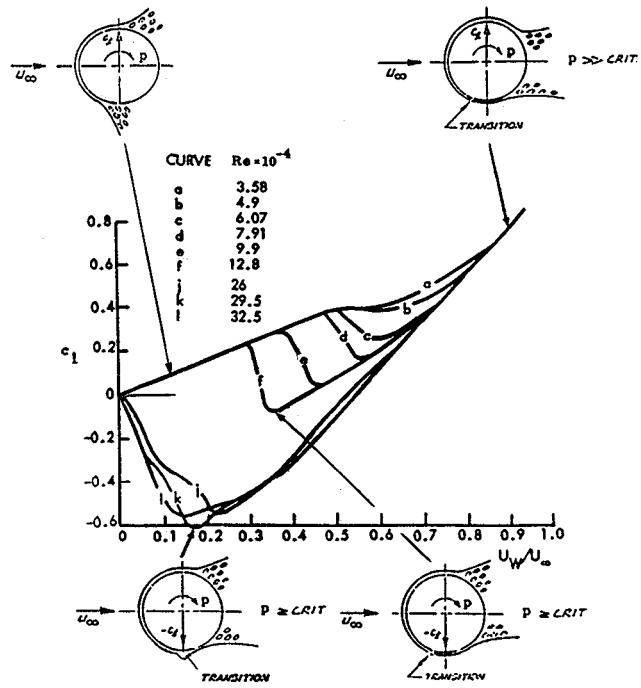

Fig. 4 Magnus lift characteristics for transitional and laminar Reynolds numbers.[19]

the crossflow conditions are near critical already in the static case (curves j, k, and l in Fig. 4).

Initially, flow asymmetry or surface irregularities set the vortex asymmetry in Fig. 5. The resulting coning motion reinforces the effects of the asymmetry, as the laminar separation is delayed on the advancing side. Positive coning velocity and acceleration result ($\dot{\psi}$ and $\ddot{\psi} > 0$). However, as $\dot{\psi}$ increases, the moving wall effect eventually causes boundary-layer transition forward of flow separation on the retreating side. This reverses the vortex asymmetry (as in the case of the Magnus lift reversal in Fig. 4), and the coning motion starts to decelerate ($\dot{\psi} > 0$, but $\ddot{\psi} < 0$). Eventually, this results in accelerated coning in the opposite direction ($\dot{\psi}$ and $\ddot{\psi} < 0$). The rotation reversal moves transition back into the wake on the new advancing side, and asymmetric laminar separation is re-established. Eventually, transition occurs on the retreating side to cause critical/subcritical flow separation, reversing the asymmetry, and the coning motion is decelerated ($\dot{\psi} < 0$, $\ddot{\psi} > 0$). The process continually repeats itself, resulting in a self-reversing coning motion with limit rates in both directions, producing $\dot{\psi}(\alpha)$ characteristics similar to those shown in Fig. 3.

The flow mechanism producing the behavior in Fig. 5 is also the essential ingredient of the "nose-slice" phenomenon. The experimental results in Fig. 5 are for Reynolds numbers below the critical region (curves a–f in Fig. 4). When the Reynolds number is increased towards the critical range, the Magnus lift reversal occurs at lower and lower values of U_W/U_∞ (curves j, k, and l in Fig. 4). Likewise, one expects the reversal of the coning motion in Fig. 5 to occur at lower and lower coning rates, reducing the nose-slice amplitude. That is, the nose-slice or coning tendency in Fig. 5 will decrease until it is completely damped at $Re \approx Re_{crit}$. A similar damping effect can be expected to be generated by the moving wall effects on the transition region on a slender forebody.[15,22] By acting as a nose-microasymmetry,[7] the transition region controls the forebody separation/vortex asymmetry. Consequently, one expects the coupling between boundary-layer transition and the coning motion to have a damping effect on the nose-slice tendencies of slender-nose aircraft, such as the Su-27 and MiG-29, especially at high altitudes where the critical flow region can cover a significant extent of the nose. The

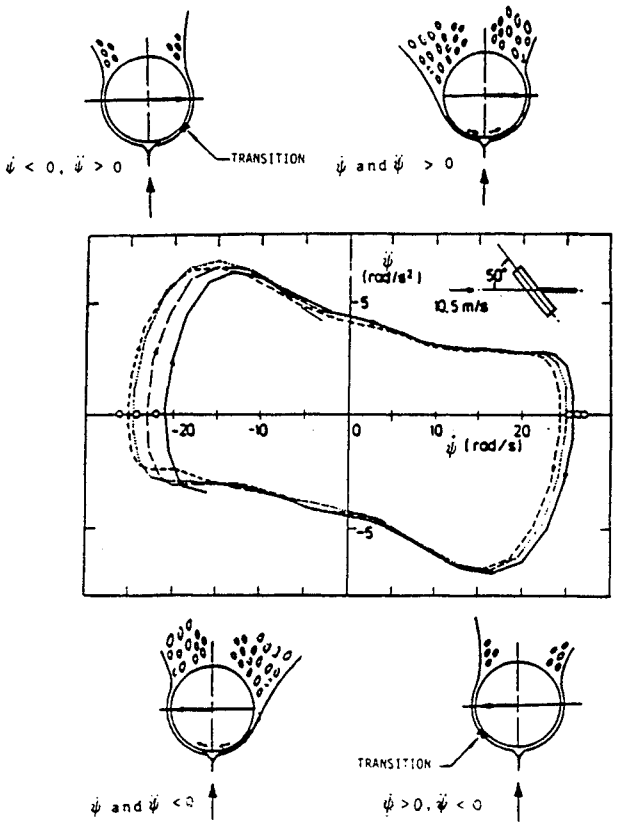

Fig. 5 Acceleration/rate time history of a coning, flat-faced, circular cylinder at $\alpha = 50$ deg for initially laminar flow conditions.[7]

critical flow region only has to be large enough to be able to switch the forebody separation asymmetry.

The results discussed above supply a sobering reminder of the fact that dynamic simulation of high-alpha vehicle dynamics is not possible unless the full-scale Reynolds number is simulated.[23,24]

Conclusions

Analysis of available experimental results leads to the following conclusions in regard to the Cobra maneuver unsteady aerodynamics:

1) In laminar flow the coupling between forebody flow separation and body motion is such that it will drive coning and nose-slice motions.

2) At full-scale Reynolds numbers the coupling between body motion and forebody boundary-layer transition is at high altitude such that coning and nose-slice motions are damped.

3) Dynamic simulation of high-alpha vehicle dynamics, e.g., in a Cobra-type maneuver, can only be simulated at full-scale Reynolds number.

References

[1]*Aviation Week*, Sept. 24, 1990, p. 32.
[2]*Aviation Week*, July 9, 1990, p. 29.
[3]Skow, A. M., "An Analysis of the Su-27 Flight Demonstration at the 1989 Paris Air Show," Society of Automotive Engineers TP 901001, April 1990.
[4]Cunningham, A. M., Jr., and Bushlow, T., "Steady and Unsteady Force Testing of Fighter Aircraft Models in a Water-Tunnel," AIAA Paper 90-2815, Aug. 1990.
[5]Manor, D., Miller, L., and Wentz, W. H., Jr., "Static and Dynamic Water Tunnel Tests of Slender Wings and Wing-Body Configurations at Extreme Angles of Attack," AIAA Paper 90-3021, Aug. 1990.
[6]McElroy, G. E., and Sharp, P. S., "An Approach to Stall/Spin Development and Test," AIAA Paper 71-772, July 1971.
[7]Ericsson, L. E., and Reding, J. P., "Asymmetric Flow Separation and Vortex Shedding on Bodies of Revolution," *Tactical Missile Aerodynamics: General Topics*, edited by M. J. Hemsch, Vol. 141, Progress in Astronautics and Aeronautics, AIAA, Washington, DC, 1991, pp. 391–452.
[8]Keener, E. R., Chapman, G. T., Cohen, L., and Taleghani, J., "Side Forces on a Tangent-Ogive Forebody with a Fineness Ratio of 3.5 at High Angles of Attack and Mach Numbers from 0.1 to 0.7," NASA TMX-3437, Feb. 1977.
[9]Ericsson, L. E., and Reding, J. P., "Alleviation of Vortex-Induced Asymmetric Loads," *Journal of Spacecraft and Rockets*, Vol. 17, No. 6, 1980, pp. 546–553.
[10]Modi, V. J., Ries, T., Kwan, A., and Leung, E., "Aerodynamics of Pointed Forebodies at High Angles of Attack," *Journal of Aircraft*, Vol. 21, No. 6, 1984, pp. 428–432.
[11]Keener, E. R., and Chapman, G. T., "Onset of Aerodynamic Side Forces at Zero Sideslip on Symmetric Forebodies at High Angles of Attack," AIAA Paper 74-770, Aug. 1974.
[12]Montevidas, R. E., Reisenthel, P., and Nagib, H. M., "The Scaling and Control of Vortex Geometry Behind Pitching Cylinders," AIAA Paper 89-1003, March 1989.
[13]Ericsson, L. E., "Unsteady Flow Separation on Slender Bodies at High Angles of Attack," *Journal of Spacecraft and Rockets*, Vol. 30, No. 6, 1993, pp. 689–695.
[14]Lamont, P. J., "The Complex Asymmetric Flow over a 3.4D Ogive Nose and Cylindrical Afterbody at High Angles of Attack," AIAA Paper 82-0053, Jan. 1982.
[15]Ericsson, L. E., "Moving Wall Effects in Unsteady Flow," *Journal of Aircraft*, Vol. 25, No. 11, 1988, pp. 977–990.
[16]Yoshinaga, T., Tate, A., and Inoue, K., "Coning Motion of Slender Bodies at High Angles of Attack in Low Speed Flow," AIAA Paper 81-1899, Aug. 1981.
[17]Dexter, P. C., "Final Report on an Analysis of the Data Obtained from Low Speed Wind Tunnel Tests of Three Calibre Tangent-Ogive Nose and Cylinder Combination at High Angles of Incidence," Bristol Aerospace, Dynamics Group, Rept. BT 15034, Bristol, England, UK, July 1983.
[18]Ericsson, L. E., "Circular Cylinder Response to Karman Vortex Shedding," *Journal of Aircraft*, Vol. 25, No. 9, 1988, pp. 769–775.
[19]Swanson, W. M., "The Magnus Effect: A Summary of Investigations to Date," *Journal of Basic Engineering*, Vol. 83, Sept. 1961, pp. 461–470.
[20]Ericsson, L. E., "Prediction of Slender Body Coning Characteristics," *Journal of Spacecraft and Rockets*, Vol. 28, No. 1, 1991, pp. 43–49.
[21]Ericsson, L. E., "Lateral Oscillations of Sting-Mounted Models at High Alpha," *Journal of Spacecraft and Rockets*, Vol. 27, No. 5, 1990, pp. 508–513.
[22]Keener, E. R., "Flow-Separation Patterns on Forebodies," NASA TM-86016, Jan. 1986.
[23]Ericsson, L. E., and Reding, J. P., "Scaling Problems in Dynamic Tests of Aircraft-Like Configurations," Paper 25, AGARD-CP-227, 1978.
[24]Ericsson, L. E., "Effects of Transition on Wind Tunnel Simulation of Vehicle Dynamics," *Progress in Aerospace Sciences*, Vol. 27, 1990, pp. 121–144.